



Integrated Geophysical Investigation using Aero-radiometric and Electrical Methods for Potential Gold mineralization within Yauri/Zuru Schist Belts, Kebbi State NW Nigeria

Abdulrahman Idris Augie¹, Kazeem Adeyinka Salako², Andy Anderson Bery³, Adewuyi Abdulwaheed Rafiu², Mufutau Owolabi Jimoh²

1. Department of Applied Geophysics, Federal University Birnin Kebbi, Nigeria

2. Federal University of Technology Minna, Nigeria

3. School of Physics, Universiti Sains Malaysia, 11800 USM, Penang, Malaysia

ABSTRACT

This study used aero-radiometric, 2D electrical resistivity tomography (ERT), and induced polarization (IP) methods to delineate gold mineralization potential. The study also confirmed and followed-up on regions with major structural features identified in previous aeromagnetic studies in the area. A half-degree airborne radiometric data of sheet 118_Yelwa from the NGSA, which contains three radioelements (%K, eTh, and eU) were used in this study. These datasets were processed and analyzed with Oasis Montaj Grid Math expression builder to obtain the %K_ratio_eTh and Ternary grid anomalies. The results identified zones E and F as hydrothermally altered regions that may harbour gold mineralization. These findings were consistent with the regions of major structural features identified in previous aeromagnetic studies in the area. The zones were located in the eastern parts of Ngaski, Yauri (Yelwa), Shanga, and Agwara, as well as Magama's northwest region. However, zone F1 (the eastern portion of Ngaski/Yauri) has been further investigated using 2ERT and IP detailed geophysical methods in a dipole-dipole configuration. The results of geoelectric techniques along profiles 1, 2, and 3 identified the major gold mineralization potential zones, which were labeled A1, A, and C. These regions have low/high resistivity and chargeability signatures, and could thus be interpreted as potential target zones for metallic mineral exploration, particularly gold mineralization. The regions are located in the northern part of Mararraba and southwest of the Jinsani areas of Kebbi State.

Keywords: Gold mineralization Zones, Yauri/Zuru Schist Belt, Aero-radiometric, Electrical Resistivity Tomography (ERT) and Induce Polarization (IP).

Investigación geofísica integrada de prospección aerorradiométrica y métodos eléctricos para definir el potencial de mineralización aurífera en el cinturón de esquistos de Yauri/Zuru, en el estado de Kebbi, en el noroeste de Nigeria

RESUMEN

Este estudio utiliza los métodos de prospección aerorradiométrica, tomografía 2D de resistividad eléctrica (ERT), y polarización inducida (IP) para delinear el potencial de mineralización aurífera en el estado de Kebbi, al noroeste de Nigeria. Este trabajo también confirmó e hizo seguimiento a estudios con características estructurales identificadas en previos análisis aeromagnéticos en el área. Con este fin se utilizaron datos radiométricos aerotransportados de medio grado de la pestaña 118_Yelwa, de la Agencia de Estudios Geológicos de Nigeria, la cual contiene tres radioelementos (%K, eTh, y eU). Estos conjuntos de datos fueron procesados y analizados con el software de expresiones matemáticas Oasis Montaj Grid Math para obtener las anomalías de la red %K_ratio_eTh y Ternary. Los resultados identificaron las zonas E y F como regiones hidrotérmicamente alteradas que podrían albergar mineralizaciones auríferas. Estos hallazgos son consistentes con las regiones de mayores características estructurales identificadas en previos estudios aeromagnéticos en el área. Estas zonas corresponden con las partes del este de Ngaski, Yauri (Yelwa), Shanga y Agwara, al igual que con la región noroeste de Magama. Sin embargo, la zona F1 (la parte más al este de Ngaski/Yauri) fue investigada más detalladamente con los métodos ERT e IP en una interacción dipolo-dipolo. Los resultados de las técnicas geoelectricas en los perfiles 1, 2 y 3 identificaron las zonas de mayor potencial de mineralización aurífera, las cuales fueron etiquetadas como A1, A, y C. Estas áreas tienen características de alta/baja resistividad y cargabilidad, por lo que podrían interpretarse como zonas potenciales para la exploración de minerales metálicos, particularmente de mineralización de oro. Estas regiones se ubican en el norte de Mararraba y en el sudoeste de Jinsani, estado de Kebbi.

Palabras clave: zonas de mineralización aurífera; cinturón de esquistos Yauri/Zuru; prospección aerorradiométrica; tomografía 2D de resistividad eléctrica; polarización inducida

Record

Manuscript received: 13/12/2023

Accepted for publication: 16/07/2024

How to cite this item:

Augie, A. I., Salako, K. A., Bery, A. A., Rafiu, A. A., & Jimoh, M. O. (2024). Integrated Geophysical Investigation using Aero-radiometric and Electrical Methods for Potential Gold mineralization within Yauri/Zuru Schist Belts, Kebbi State NW Nigeria. *Earth Sciences Research Journal*, 28(2), 137-146. <https://doi.org/10.15446/esrj.v28n2.112066>

1. Introduction

In Nigeria, gold occurs primarily in quartz veins as well as an accessory mineral in metasedimentary and meta-igneous rocks across the schist belt stratum (Ramadan and Abdel-Fattah, 2010). The Nigerian gold fields have witnessed extensive artisanal work, with a concentration on both major gold-quartz reefs and their associated alluvial occurrences (Garba, 2000; Sani et al., 2019). Geophysical studies are required to generate a database of precise coordinates as well as to identify the zones containing these gold minerals (Au). Au is typically found in hydrothermal deposits in the uppermost portion of the continental crust of Earth and it is the most noble chemical element (Frimmel and Gartz, 1997).

Many geophysical studies, both qualitative and quantitative, were conducted in the research area in an attempt to identify mineralization potential zones. Bonde et al. (2019) and Lawali et al. (2020) carried out analyses on aeromagnetic data over the study area with the goal of identifying structural potential mineralization zones. Analytic signal (AS), first vertical derivatives (FVD), second vertical derivatives (SVD), and tilt derivatives (TDR) are the enhancing filters used in the research. The study resulted in identification of structures with a NE-SW direction like as fracture as well as faults, and veins, in which economic minerals usually hosted. The literature, however, includes gaps because the study entirely relied on aeromagnetic data gathered from secondary sources. The anomalous zones revealed by aeromagnetic investigations were not followed up on with detailed studies such as 2D electrical resistivity imaging (ERI) and induced polarization (IP) geophysical techniques.

Aisabokhae (2021) and Lawal et al. (2021) used aeromagnetic and aeroradiometric datasets to study possible mineralization zones of the Kebbi south. The following enhancement filtering techniques were utilized in the study: reduction to the magnetic equator (RTE), AS, FVD, Euler deconvolution (ED), composite image, ratio maps, and ternary image. According to the conclusions of the study, the Anka schist region is located on the edge of a plutonic area exhibiting brittle-ductile distortion, signifying structural fracture for fluid flow and associated alteration caused by hydrothermal occurrences toward mineralization in the regions. However, there are gaps in the literature as the authors did not effectively use the magnetic equator to centralise the anomalies because the study area is within equatorial zones of low latitude. At these regions, a further amplitude correction is frequently required to prevent the data's north-south signal from dominating the results according to Holden et al. (2008), Core et al. (2009). The anomalous zones identified in the research were not further examined utilising detailed methods such as 2D ERT and IP geophysical methods for the identification of mineralised potential zones.

However, Augie et al. (2021, 2022a & b) analysed the magnetic signatures in combination with the geological context of the area, to determine the structures that could host gold mineralization across Kebbi South. The following techniques were used in the study: RTE, FVD, SVD, CET, TDR, ED, SPI and 2D magnetic modelling. These techniques' results aided in the delineation of lineaments like as faults, fractures, especially shear zones thought to be related with alteration zones, which play a significant part in defining gold mineralised prospect. When contrasted with the geological setting of the area, the structures delineated within it correlate to the regions underlain by the following earth materials; granite, gneiss, quartz-mica schist, biotite diorite, biotite hornblende granite and medium coarse-grained. Results of these techniques identified alteration zones that could host gold mineralization zone. These potential zones' locations correspond to the SE portions of Yelwa (Yauri) as well as Shanga, Magama, Fakai, Rijau, Zuru, Ngaski, and the eastern parts of Bukkuyum and Wasagu/Danko.

In this study, aero-radiometric, 2D ERT and IP methods were employed to delineate gold mineralization potential. The aero-radiometric approach was utilised to identify the hydrothermal alteration zone that could potentially hold gold mineralization potential, as well as to support the results with previous aeromagnetic studies (Augie et al., 2022a&b) of the area. The airborne radiometric technique revealed hydrothermally altered zones, which were then explored for potential gold prospects and associated mineralization using 2D ERT and IP geophysical methods.

1.1 The study Area

The research area is located within southern Kebbi and some portions of Niger state. It is bounded by latitudes 10°30'0"N and 11°0'0"N, and longitudes

4°30'0"E and 5°0'0"E. The area includes the following local government areas (LGAs): the SE part of Yauri, Ngaski, Shanga, Magama, and Agwara areas (Fig. 1). Geologically, the area lies within the basement complex regions of northwestern Nigeria. The area is underlain by Mangrove Swamps, Gwandu Formation, Nupe Sandstone and Pan-African Older Granitoid (Garba, 2000; 2003). These comprised; Sands, Clays, Sandstones, Siltstones, and Undifferentiated Schists including Phyllite, Medium to Coarse-Grained Biotite, Migmatitic Augen Gneiss and Granite Gneiss as shown in Figure 1.

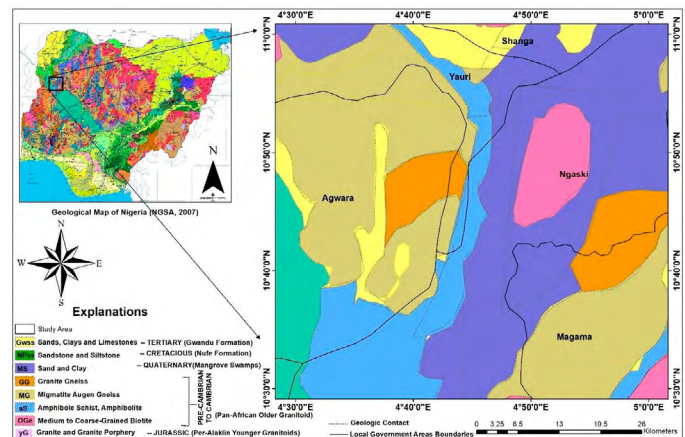


Figure 1. Geological map of the study area (modified after NGSA, 2007)

2. Methods

2.1 Acquisition and Processing of Airborne Radiometric Data

A half degree sheet of aero-radiometric data of the research region was obtained from the Nigerian Geological Survey Agency (NGSA). The sheet 118_Yelwa was used in the study which comprised some portion of; Yauri (Yelwa), Ngaski, Shanga and Agwara as shown in Fig. 1. These data were collected by Fugro airborne survey on behalf of the NGSA of the Federal Government of Nigeria between 2005 and 2009 (Augie et al. 2022a). The data were collected at an altitude of 100 meters, with a flight line spacing of 500 meters aligned NW-SE and a tie line spacing of 2000 meters. The maps of this grid data sheet have a scale of 1:100,000 as well as half-degree sheet.

The acquired gridded data which contain the concentrations of Potassium (K) as well as equivalent Thorium (eTh) and Uranium (eU) were input into a Geosoft "Oasis Montaj Software" to process each radio-element. Each of these elements were blended independently using the blending technique provided by the Grid and Image geosoft extension (GX) to obtain anomalous concentration grids for the three elements (%K, eTh, and eU). The Potassium Ratio Thorium (%K_ratio_eTh) grid anomaly was also developed with the aid of the Grid Math expression builder of the Oasis Montaj using Equation 1.

$$G_0 = \frac{G_1}{G_2} \quad (1)$$

Following that, using the blending method in Grid and Image of GX, the total count map integrating the combined effects of ^{40}K , ^{238}U , and ^{232}Th was obtained. These were then utilized to come up with the ternary map, which consisted of different colours that corresponded to every of the radioelement abundances. The colour red was assigned to the %K., green as eTh, and blue as eU (Milligan & Gunn, 1997) and each of the three-radioelement concentration in the red, green, and blue colors were then merged using Grid and Image GX of Oasis Montaj. The ternary map has been developed to identify radioelement variations associated with hydrothermal alteration zones that could be favourable for gold mineralization. Radioelement content in host rocks can vary as a result of hydrothermal processes. Of the three radioelements, potassium (K) is affected by these processes the most, whereas thorium (Th) is affected less frequently and uranium (U) only rarely. Potassium levels often rise

during signature alterations, but weathering typically reduces the intensity of signature alterations. Mineralising hydrothermal fluids is usually associated with potassium to source rocks (Tawey et al., 2021). It may be hosted by potassium feldspar or muscovite, and prospective outcropping or sub-cropping mineralization can be identified by an increase in K counts during a radiometric survey (Dickson and Scott, 1997).

2.2 2D Geoelectric Prospecting Method

In this study, a 2D geoelectrical survey was also carried out at Yauri/ Ngaski boundaries of Kebbi state, NW Nigeria. An area 640 m² of fields were investigated using a dipole-dipole configuration with minimum electrode spacing (*a*) of 10.00 meters. A total of 3 profiles were designed for each 300 m distance along the profile, oriented NW-SE (Fig. 2).

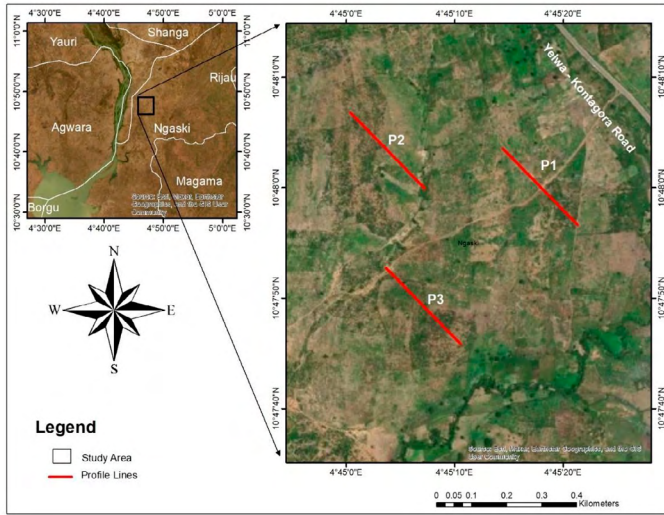


Figure 2. Profile line field survey layout

The data was collected using a Super Sting (resistivity meter) connected to an electrode selector and supplied by a 12 V battery. This instrument has the capability of measuring apparent resistivity and IP data simultaneously. It is equipped with a transmitter with automatic/user configurable currents in milliamps; 1, 2, 5, 10, 20, 50, 100, 200, 500 and 1000 mA. The distance between the two pairs of current electrodes (C1 and C2) was chosen to be equal to the distance between the two potential electrodes (P1 and P2). The distance between C1 and P1 (dipole separation factor) was calculated as a multiple of an integer *n* of the distance between the C1-C2 and P1-P2 (Fig. 3).

The dipole separation factor *n* was initially set to one (1), then increased to two (2), three (3), and so on until it reached a maximum value of eight (8). Thus, the two-parameter; dipole separation factor (*n*) and the space between the current electrode pair (*a*) have been measured. The measurements were taken with electrode separation of 10 m and *n* was set at 1, 2, 3, up to 8 (Fig. 3). The more the increase in *n* which would equally increase the electrode spacing as well as more the injected current flows to greater depths (Loke, 2000).

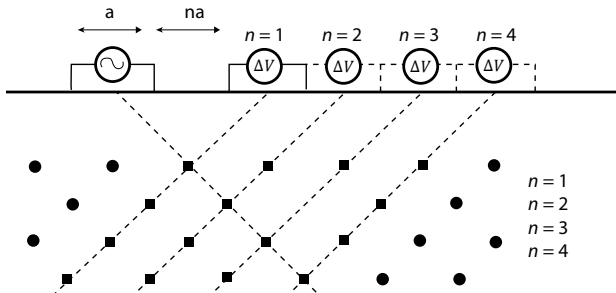


Figure 3. Illustration of dipole-dipole array pseudo-section when putting the measured values (Wahyu, 2016)

Electrodes 1, 2, 3, and 4 (C1, C2, P1 and P2) were used for the initial measurement. C2 was employed at 0 m, C1 at 10 m, P1 at 20 m, and C2 at 30 m. Likewise, in the second measurement, C2 at 10 m, C1 at 20 m, P1 at 30 m, and P2 at 40 m respectively. These procedures were repeated down the profile line using 1*a*, 2*a*, 3*a*, 4*a*, 5*a*, 6*a*, 7*a*, and 8*a* spacing between C1 and P1 where *a* is 10 m. At each measurement, the measured ground apparent resistivity and IP values were obtained. The obtained data were analyzed using Loke (1999)'s RES2DINV programme, which automatically produces 2D resistivity and IP models for the subsurface.

3. Results

3.1 Results from Aero-radiometric Technique

Figure 4 depicts a ratio map of %K/eTh concentration that shows zones of hydrothermally altered zones which usually lead to radioactive element enrichment. In general, thorium (eTh) is unaffected by alteration activities since it is often dormant in mineral content processes, or It might as well be reduced in zones of high %K as well as silicification (Lundien, 1967). The %K/eTh ratio map indicates that a high Potassium content in the red colour indicates a low Thorium level as well as a high Thorium concentration in the blue colour indicates a Potassium level. The summarized results of the colour compositions for K/Th versus radioelements were given in Table 1.

Zone E has a high concentration of K/Th concentrations (enrichment in K) and is found in the following areas: the eastern part of Yauri, Shanga, Ngaski and Agwara, and the northwest parts of Magama. These areas are substantial hydrothermally altered zones indications having the anomalous of the enrichment in K range of 0.199 to 0.443 ppm. However, many literatures (such as Durrance, 1986; Dickson and Scott, 1997), revealed that the alteration environment as revealed in Fig 4, may typically accumulate various mineralization potential, particularly gold minerals. This is due to hydrothermal solutions having ability of decomposing and conveying many different types of minerals and metallic substances, which are crucial in mechanisms of ore deposition, particularly metallic minerals (Hoover and Pierce, 1990).

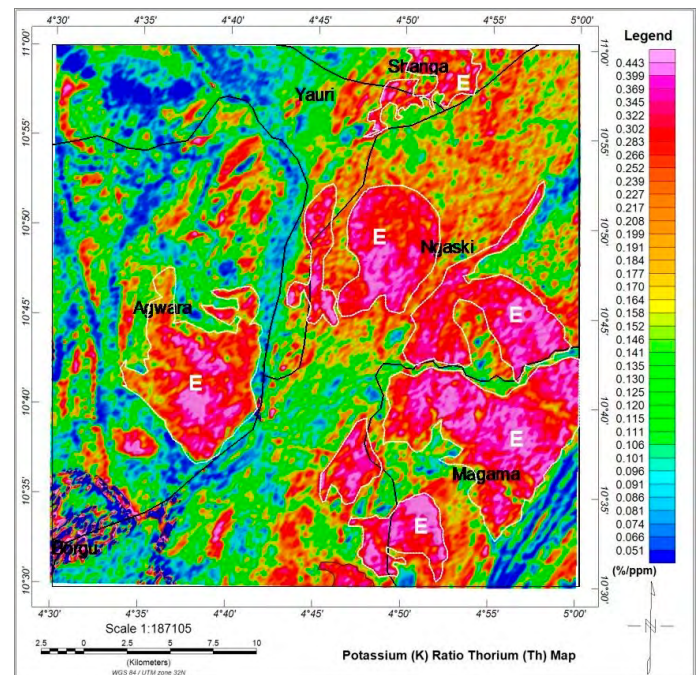


Figure 4. K/eTh map of the study area

Figure 5 depicts a ternary map of radioelements (%K, eTh and eU) with a variety of colour combinations. Table 2 summarizes the results for Figure 5 in terms of colour composition versus radioelements. The Red colour indicates a high %K with a low eU and eTh, Blue shows a rich concentration of eU having a low %K as well as eTh. Green exhibited a high concentration of eTh

alongside a low %K and eU. Cyan denotes a high eTh and eU with a low %K, Magenta defines a high %K as well as eU having a low eTh, Yellow signifies a high %K with eTh but a low eU, Black represents a low %K, eTh, as well as eU, and White denotes a high %K, eTh, and eU. Many literatures (such as Hoover and Pierce, 1990; Ohioma et al., 2017; Lawal et al., 2021; Adetona et al., 2022; etc.) discovered that aero-radiometric surveying techniques of radioelements that could mark gold deposits are variable, with potassium being the most reliable guide.

Using the colour scheme shown in Fig. 5, the region that exhibits Blue, Green, Cyan, Yellow, and Black indicates very low potassium concentrations, implying that hydrothermal alteration did not occur in this zone of K. Zone F, on the other hand, has a very low concentration (0.051 to 0.146 ppm) of uranium (eU) and thorium (eTh) while having a high concentration (0.199 to 0.443 ppm) of potassium (%K), which corresponds with the high %K/eTh in the E region of the %K/eTh ratio map shown in Figure 4. These regions are situated in the eastern parts of Ngaski and Agwara, as well as the northwest parts of Magama. The overabundance of potassium in comparison to the other elements, especially thorium, implies hydrothermal alteration. These are the hydrothermal alteration regions that could potentially be favourable for gold mineralization. The hydrothermally altered zones (F1 in particular) identified by the aero-radiometric technique were investigated further using 2D ERT and IP detailed geophysical methods.

The summary of the results of aero-radiometric techniques: colour compositions versus radioelement concentrations based on Figures 4 and 5 are given on Table 1 and 2.

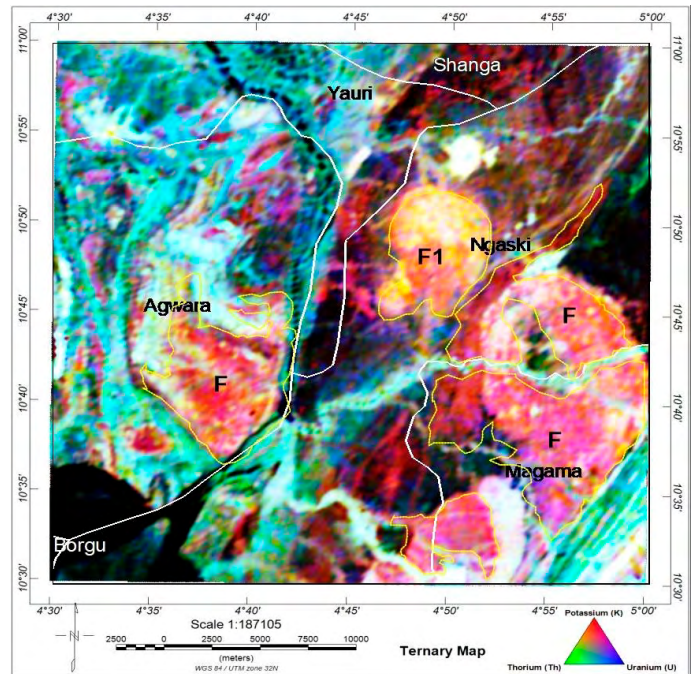


Figure 5. Ternary map of K, eTh, and eU of the study area.

Table 1. Concentrations of K/eTh versus colour compositions of the area

S/No	Concentrations of radioelements	Enrichment in radioelements (ppm)	Colour compositions for %K ratio eTh	Location	Province and Country	Probable gold and other mineralization potential remarks
1.	High %K and low eTh	0.199 to 0.443	Red	Eastern part of Yauri, Shanga, Ngaski and Agwara, and the northwest parts of Magama	NW Nigeria	Yes
2.	Moderate %K and moderate eTh	0.111 to 0.198	Yellow and green	NE part of Ngaski and SW part of Ngaski	NW Nigeria	No
3.	Low %K and high eTh	0.051 to 0.101	Blue	Western parts of Yauri and Agwara	NW Nigeria	No

Table 2. Ternary images of K, eTh, and eU versus colour compositions of the area

S/No	Concentrations of radioelements	Colour compositions for %K, eU and eTh	Location	Province and Country	Probable gold and other mineralization potential remarks
1.	High %K, low eU and low eTh	Red	Eastern part of Yauri, Shanga, Ngaski and Agwara, and the northwest parts of Magama	NW Nigeria	Yes
2.	High eU, low %K and low eTh	Blue	NE part of Agwara	NW Nigeria	No
3.	High eTh, low %K and low eU	Green	SE part of Magama and western parts of Yauri and Agwara	NW Nigeria	No
4.	High eTh, high eU and low %K	Cyan	Western parts of Yauri and Agwara	NW Nigeria	No
5.	High %K, high eU and low eTh	Magenta	Shanga and NE part of Ngaski	NW Nigeria	No
6.	High %K, high eTh and low eU	Yellow	Eastern part of Borgu and Northern part of Magama	NW Nigeria	No
7.	Low %K, low eTh and low eU	Black	Borgu and Eastern part of Ngaski	NW Nigeria	No
8.	High %K, high eTh and high eU	White	SW part of Magama and Central part of Agwara	NW Nigeria	No

3.2 Results from 2D Geoelectric Prospecting Techniques

The interpretation of the 2D geoelectric modelled sections is associated with the geological setting of the area. These include the borehole lithology of the southern part of Kebbi as revealed by Rural Water Supply and Sanitation Agency (RUWASA) and resistivity values (Osazuwa and Chii, 2010) in Table 3. These adjoining borehole logs were obtained from previous works and subsequently used to correlates the findings of the present study.

Table 3. A borehole/lithology log of the southern part of Kebbi areas (SARDA, 1988; Osazuwa and Chii, 2010)

Lithology	Depth(m)	Thickness(m)	Resistivity range (Ω m)
Lateritic Sand	0-2	2	60-1000
Highly Decomposed Schist	2-10	8	10-500
Partially Decomposed Granite	10-15	12	100-1000
Quartzite's and Gneiss	15-21	16	200-100000

3.2.1 Geoelectric Sections for Profile 1

Figure 6(a) is the 2D inverse model section for profile 1. It is oriented in the NW-SE direction and has a lateral distance of 300 m. The profile lies between latitudes 10°48'3.6"N to 10°47'56.4"N and longitudes 4°45'14.4"E to 4°45'21.6"E (Fig. 2). The subsurface feature was sectionalised into four different zones namely: A, B, C, and D. Zone A is characterized by resistivity values ranging from 1.6 Ω m to 459 Ω m, and are located on 10-80 m, 190-200 m, 250-265 m along the profile and a depth/thickness of 12.0

m, 18.5-24.9 m and 7.5-18.5 m respectively. Zone B has resistivity values of 460 Ω m to 1888 Ω m, it covers a length of 30-110 m, 130-149 m, 190-200 m and 245-265 m at a corresponding depth/thickness of 2.5-18.5 m, 24.9 m, 18.5 m and 2.5-18.5 m. Zone C is characterized by resistivity values going from 1889 Ω m to 7773 Ω m, it covers the distance along the profile of 35-55 m, 70-92 m, 105-130 m, 145-180 m, 200-210 m and 220-270 m and a depth/thickness of 8-24.9 m, 3-24.9 m, 24.9 m, 24.8 m, 24.9 m and 7.5 m. Likewise, zone D is portrayed by the resistivity of 7774 Ω m to 32002 Ω m, it has occupied a length of 100-125 m, 175-190 m, 200-250 m and 265-290 m at a corresponding depth/thickness of 7.5-24.9 m, 12-24.9 m, 2.5-24.9 m and 18.5 m respectively.

The subsurface lithology for features A, B, C, and D as compared with Table 3 could be lateritic soil, highly decomposed schist, partially decomposed granite and quartzite, and quartzite/gneiss. However, zone A of low resistivity areas could result from water content and enduring in the oxidized rock. Some minerals, especially gold, could be associated by this kind of oxidized rock that originates from granite. The younger granite phases in region, was thought to be the origin of the gold mineralization (Bagare et al., 2018 and 2019). Zone C is associated with partially decomposed granite and quartzite which form dykes. Dyke subsurface structures of the aforementioned rock formation could be crucial in detecting the gold mineral. The results of the inverse model section given in Figure 6(a) were further transformed into a geologic section as shown in Figure 6(b).

The results of 2D inverse model chargeability sections along profile 1 (IP1) are given in Figure 7. The sections revealed clearly the regions that exhibit metallic minerals namely zone A1. These regions have the most noteworthy chargeability values ≥ 20 msec. It covers an x-position of 45-60 m, 190-202 m and 202-255 m at a corresponding depth/thickness of 7.5-18.5 m, 7.5 m and 12.8-24.9 m. The higher chargeability of zone A1 generally happens because of the collection of metallic minerals in host rocks. These locales could be considered as a possible objective for the investigation of specific metallic minerals, particularly gold mineralization.

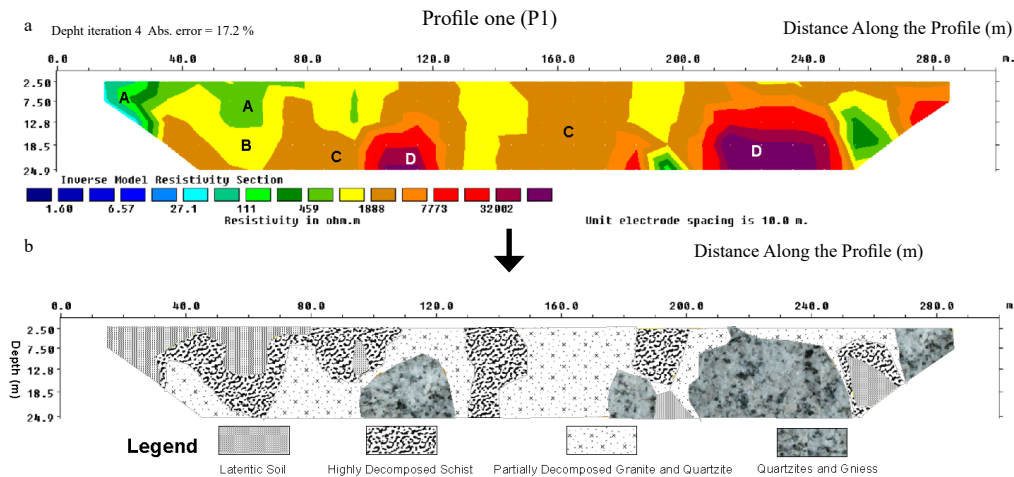


Figure 6. (a) Inverse model resistivity section and (b) geologic section of profile one (P1)

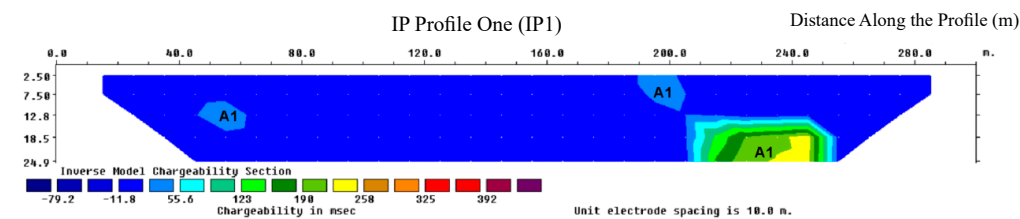


Figure 7. Inverse model chargeability section for profile one (IP1)

3.2.2 Geoelectric Sections for Profile 2

Profile 2 has a lateral extent of 300 m (Fig. 8). It is oriented NW-SE and is located between latitudes 10°48'7.2"N to 10°48'0"N and longitudes 4°45'0"E to 4°45'7.2"E (see Fig. 2). The subsurface resistivity differences were classified as zones A, B, C, and D. Table 2 summarises the subsurface variations for these zones in relation to resistivity of common rocks as well as borehole lithology of the area as given in Table 3.

The zones of low and high resistivity (A and C) were discovered to be the key zones of probable gold mineralization. According to the geological setting of the research region, the low resistivity zone (A) could be the result of weathering in an oxidised rock, and these rock types are generally granite or rhyolite in origin. As a result, it may be associated with some minerals, particularly gold and other metallic minerals. However, the dyke structures of granite and quartzite were generated by a high resistivity zone (C). These structures could be crucial in identifying mineralization potential, particularly gold minerals. These findings led to the creation of the geologic section depicted in Figure 8(b).

Figure 9 depicts the results of the 2D inverse model chargeability section for profile two (IP2). The sections of this profile clearly highlighted the regions with mineralization potential, which was zone A1. These areas tend to have a higher chargeability, which could be due to the accumulation of metallic minerals in host rocks such as altered hydrothermal veins and granite. Table 4 provides the lateral distances and depths occupied by the zones. These locations could be regarded as prospective targets for investigating explicit metallic minerals, particularly gold mineralization.

3.2.3 Geoelectric Sections for Profile 3

The 2D resistivity model section along profile 5 is given in Figure 10(a). It covers a lateral distance of 300 m and lies between latitudes 10°47'52.8"N to 10°47'45.96"N and longitudes 4°45'3.6"E to 4°45'10.8"E (see Fig. 2). The subsurface resistivity signature was categorised as zones A, B, C, and D based on the resistivity of the rock formation and the geological setting of the area. The suggested subsurface lithology for features A, B, C, and D are given in Table 3.

Zone A is associated with oxidized granite/quartzite and gneiss, and it could usually be associated with certain minerals, particularly gold and other metallic minerals, based on geological contexts and the resistivity of common rocks (Table 3). Zone C, which developed the dyke structures associated with partially decomposed granite and quartzite, is another promising zone for metallic minerals. These structures may be crucial in determining mineralised zones, notably gold mineralization. The results of the profile, have led to the creation of the geologic section depicted in Figure 10(b).

Figure 11 shows chargeability sections along profile three (IP3). Zone A1 indicated the sections with the highest chargeability. Higher chargeability in zones A1 (70 msec and above) may arise due to the presence of metallic minerals. Table 4 summarises the length and depth of these zones. These areas of the highest chargeability could be regarded as an expected target for the exploitation that led to the exploration of gold mineralization in the regions.

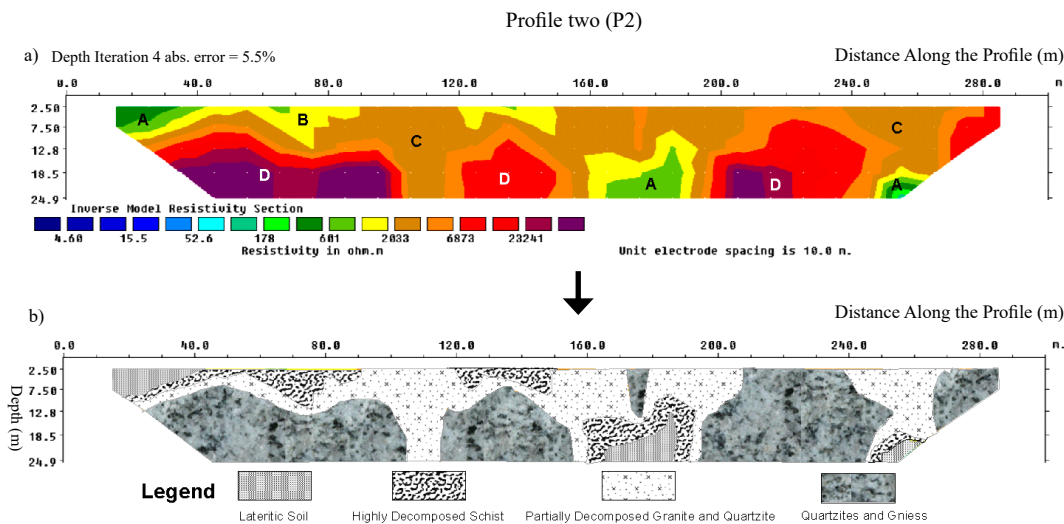


Figure 8. (a) Inverse model resistivity section and (b) geologic section of profile two (P2)

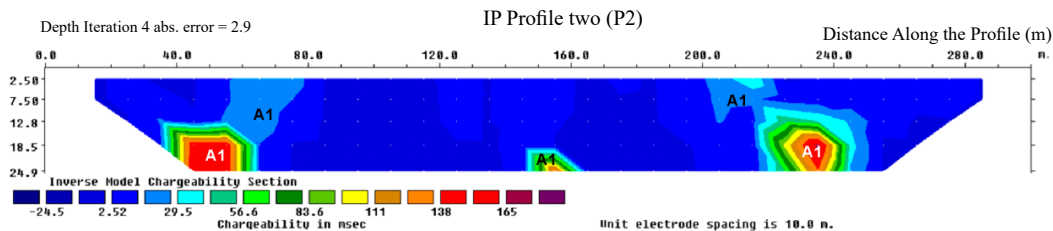


Figure 9. Inverse model chargeability section for profile two (IP2)

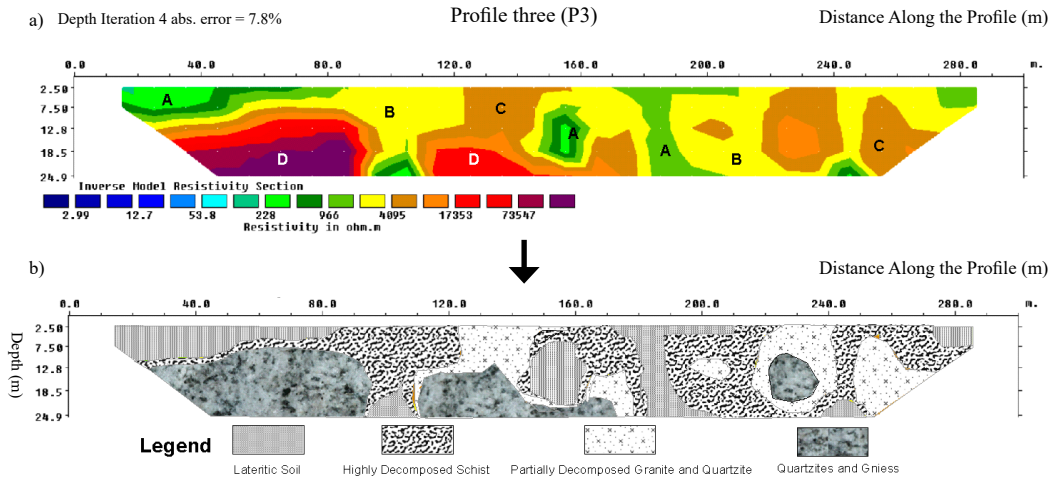


Figure 10. (a) Inverse model resistivity section and (b) geologic section of profile three (P3)

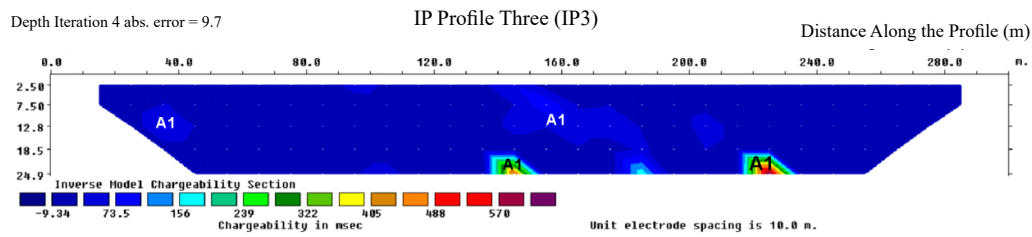


Figure 11. Inverse model chargeability section for profile three (IP3)

Table 4. Summary of results obtained from the integrated methods

Profile	Resistivity Results				Induced polarization Results				Probable gold mineralization potential remarks
	Zone	Resistivity ranges (Ω m)	Lateral lengths (m)	Depth/3 Thickness (m)	Zone	Chargeability ranges (msec)	Lateral lengths (m)	Depth/ Thickness (m)	
P1	A	1.6 to 459	10-80, 190-200 and 250-265.	12.0, 18.5-24.9 and 7.5-18.5	A1	≥ 20	45-60, 190-202 and 202-255	7.5-18.5, 7.5 and 12.8-24.9	Yes
	B	460 to 1888	30-110, 130-149, 190-200 and 245-265	2.5-18.5, 24.9, 18.5 and 2.5-18.5	-	-	-	-	No
	C	1889 to 7773	35-55, 70-92, 105-130, 145-180, 200-210 and 220-270	8-24.9, 3-24.9, 24.9, 24.8, 24.9 and 7.5	-	-	-	-	Yes
	D	7774 to 32002	100-125, 175-190, 200-250 and 265-290	7.5-24.9, 12-24.9, 2.5-24.9 and 18.5	-	-	-	-	No
P2	A	4.6 to 601	5-40, 165-185, 245-260	7.5, 18.5-24.9 and 18.5-24.9	A1	20 and above	35-65, 55-80, 145-160, 200-220 and 221-250	12.8-24.9, 12.8, 18.5, 7.5 and 7.5-24.9	Yes
	B	602 to 2033	40-90, 120-150, and 155-190	12, 7.5 and 18.5-24.9	-	-	-	-	No
	C	2034 to 6873	10-90, 95-120, 140-170, 180-205, 240-270	2.5-12.8, 24.9, 12.8, 12.8 and 18.5	-	-	-	-	Yes
	D	6874 to 23241	10-105, 115-155, 170-180, 200-245, and 270-290	7.5-24.9, 7.5-24.9, 12.8, 24.9 and 18.5	-	-	-	-	No

(Continued)

Profile	Resistivity Results				Induced polarization Results				Probable gold mineralization potential remarks
	Zone	Resistivity ranges (Ωm)	Lateral lengths (m)	Depth/3 Thickness (m)	Zone	Chargeability ranges (msec)	Lateral lengths (m)	Depth/ Thickness (m)	
P3	A	2.99 to 966	5-80, 90-105, 135-160, 170-190, 235-50 and 270-290	7.5, 18.5-24.9, 7.5-18.5, 24.9, 18.5-24.9 and 7.5	A1	70 and above	30-45, 135-150, 140-170 and 210-240	7.5-18.5, 18.5-24.9, 2.5-18.5 and 18.5	Yes
	B	967 to 4095	10-90, 91-120, 145-180, 190-220 and 240-270	3-7.5, 18.5, 12.8, 24.9, and 18.5	-	-	-	-	No
	C	4096 to 17353	120-150, 160-175, 195-210, 220-240 and 250-270	12.8, 18.5-24.9, 12.8-18.5, 19 and 7.5-24.9	-	-	-	-	Yes
	D	17354 to 73547	10-90, 110-170 and 220-235	7.5-24.9, 12.8-24.9 and 12.8-18.5	-	-	-	-	No

Table 5. Generated database of the potential gold mineralised zones in the study area

Profile No.	Lateral lengths (m)	Depth/ Thickness (m)	Geographic coordinate.				Locations
			Left End		Right End		
			Longitude	Latitude	Longitude	Latitude	
P1	10-80, 190-200, and 202-255.	18.5, 24.9, and 24.9	4°45'14.76"E, 4°45'17.64"E and 4°45'19.44"E	10°48'3.24"N, 10°48'0.36"N and 10°47'58.56"N	4°45'16.2"E, 4°45'18.36"E and 4°45'20.52"E	10°48'1.8"N, 10°47'59.64"N and 10°47'57.48"N	Mararraba
P2	35-100, 145-200, and 220-250.	12.8, 18.5 and 24.9	4°45'0.72"E, 4°45'3.24"E and 4°45'4.68"E	10°48'6.48"N, 10°48'3.96"N and 10°48'2.52"N	4°45'2.16"E, 4°45'3.96"E and 4°45'5.76"E	10°48'5.04"N, 10°48'3.24"N and 10°48'1.44"N	SW of Jinsani
P3	0-45 and 140-180.	18.5 and 28.5	4°45'3.96"E and 4°45'7.92"E	10°47'52.44"N and 10°47'48.84"N	4°45'5.04"E and 4°45'8.64"E	10°47'51.36"N and 10°47'48.12"N	SW of Jinsani

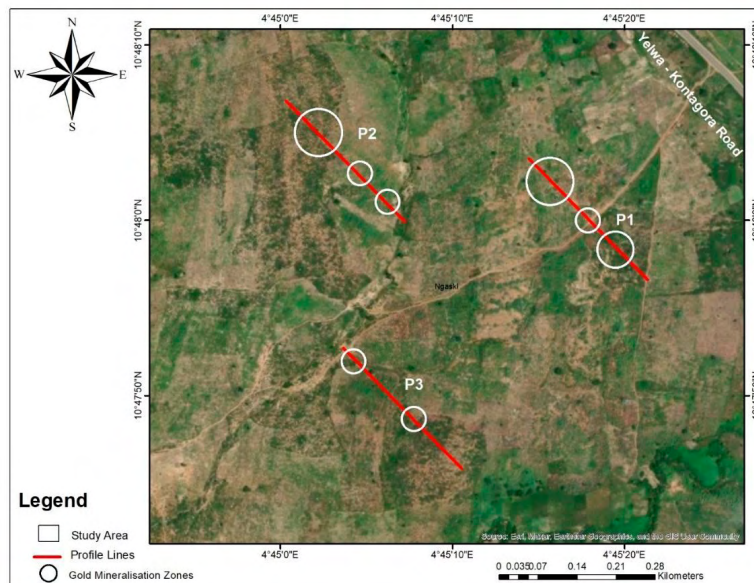


Figure 12. Major zones of gold mineralization potentials map

3.2.4 Possible Potential Gold Mineralized Zones of the Area

The suggested zones of mineralization potential along geoelectric profiles 1, 2 and 3 (P1, P2 and P3 as well as IP1, IP2 and IP3) are zones A, C and A1. These regions are characterized by low/high resistivity and high chargeability signatures as shown in Figures 6-10. Table 4 provides the integrated key zones of gold mineralization potential (Fig. 12). These zones could be inferred as a potential target for the exploration of metallic minerals, particularly gold mineralization. The results of this study led to the development of a database, which is displayed in Table 5 and contains the exact coordinates and depths of prospective gold mineralization zones. This database has the potential to enhance the region's gold exploration activities.

4. Conclusion

The use of integrated geophysical methods in this study resulted in the creation of a database containing precise coordinates, lateral lengths, and thickness/depths for potential gold mineralization zones. This database could be used to help improve gold exploration in the region. The study also supported the regions with major structural features discovered in earlier magnetic studies in the area by Augie et al. (2021) and Augie et al. (2022a,b). An aero-radiometric approach utilised in this study indicated areas of the hydrothermally altered zone that possibly host gold mineralization, and the results are in conformity with the previous findings of aeromagnetic studies within the study region. The hydrothermally altered zones (E and F) derived from airborne gamma-ray spectrometry used in this study are the eastern parts of Yelwa (Yauri), Ngaski, Shanga, Agwara, as well as the northwest parts of Magama. The zone F1 (eastern half of Ngaski/Yauri) has been further investigated using 2D ERT and IP detailed geophysical methods. The geoelectric method results along profiles 1, 2, and 3 identified the major zones of gold mineralization potential, which are zones A, C, and A1. These regions are characterized by low/high resistivity and chargeability signatures and could thus be interpreted as possible target zones for metallic mineral exploration, especially gold mineralization. These areas are located in the northern part of Mararraba and the southwest of the Jinsani areas of Kebbi State.

Data Availability

The acquired and generated datasets in the current study are not available to the general public due to the following reasons: (a) Aero-radiometric data are under the custody of the Nigeria Geological Survey Agency (NGSA) and can only be released upon request and payment via their website (<https://ngsa.gov.ng>), and (b) resistivity and induced polarization data generated in this study area are available from the corresponding author on reasonable request.

Acknowledgements

The authors would like to express their profound appreciation to the tertiary trust fund (Tetfund) for funding this research and the management of the Nigeria Geological Survey Agency (NGSA) for the release of the airborne radiometric dataset. Our thanks are also extended to the district heads of Mararraba of Yelwa Yauri area of Kebbi state for approval of the site to collect geophysical data. Their appreciation also goes to the Department of Physics, Bayero University Kano, and the Department of Geophysics, Federal University of Technology Minna for providing the instruments as well as Geosoft Inc. for the use of Oasis Montaj and Res2dinv Softwares.

Conflict of interest

The authors have no conflict of interest to disclose.

References

Adetona, A. A., Kwaghhuwa, F. I., & Aliyu, S. B. (2022). Interpreting the magnetic signatures and radiometric indicators within Kogi State, Nigeria for economic resources. *Geosystems and Geo-environment*, 2, 100157, <https://doi.org/10.1016/j.geogeo.2022.100157>

Aisabokhae, J. E. (2021). Geophysical mapping and mineralisation characterisation of the mesothermal auriferous basement complex in southern Ke-

bbi, NW Nigeria. *NRIAG Journal of Astronomy and Geophysics*, 10(1), 443-465, <https://doi.org/10.1080/20909977.2021.2005333>

Augie, A. I., Salako, K. A., Rafiu, A. A., & Jimoh, M. O. (2022a). Geophysical assessment for gold mineralization potential over the southern part of Kebbi State using aeromagnetic data. *Geology, Geophysics & Environment*, 48(2), 177-193. <https://doi.org/10.7494/geol.2022.48.2.177>

Augie, A. I., Salako, K. A., Rafiu, A. A., & Jimoh, M. O. (2021). *Estimation of depth to structures associated with gold mineralisation potential over southern part of Kebbi State using aeromagnetic data*. 3rd School of Physical Sciences Biennial International Conference Futminna 2021, Federal University of Technology Minna, 290-297.

Augie, A. I., Salako, K. A., Rafiu, A. A. & Jimoh, M. O. (2022b). Geophysical magnetic data analyses of the geological structures with mineralization potentials over the southern part of Kebbi, NW Nigeria. *Mining Science*, 29, 179-203. <https://doi.org/10.37190/msc222911>

Bagare, A. A., Saleh, M., Aku, M. O. & Abdullahi, Y. M. (2018). 2D electrical study to delineate subsurface structures and potential mineral zones at Alajawa artisanal mining site Kano state Nigeria. *Journal of the Nigerian Geophysical Society*, 1(1), 24-32.

Bagare, A. A., Saleh, M., Aku, M. O. & Abubakar, M. (2019). Geoelectrical study to determine stratigraphic setting of Alajawa artisanal mining site, Kano state, Nigeria. *Bayero Journal of Physics and Mathematical Sciences*, 10(1), 44-53.

Bonde, D. S., Lawali, S., & Salako, K. A. (2019). Structural mapping of solid mineral potential zones over southern part of Kebbi state, northwestern Nigeria. *Journal of Scientific and Engineering Research*, 6(7), 229-240.

Core, D., Buckingham, A., & Belfield, S. (2009). Detailed structural analysis of magnetic data-done quickly and objectively. *SSEG New*, 1(2), 15-21.

Dickson, B. L., & Scott, K. M. (1997). Interpretation of aerial gamma ray surveys-adding the geochemical factors. *AGSO Journal of Australian Geology and Geophysics*, 17(2), 187-200.

Dickson, B. L., & Scott, K. M. (1997). Interpretation of aerial gamma-ray surveys-adding the geochemical factors. *AGSO Journal of Australian Geology and Geophysics*, 17(2), 187-200.

Durrance, E. (1986). *Radioactivity in geology: principles and applications*. Chichester: Ellis Horwood, 441.

Frimmel, H., & Gartz, V. (1997). Witwatersrand gold particle chemistry matches model of metamorphosed, hydrothermally altered placer deposits. *Mineralium Deposita*, 32, 523-531. <https://doi.org/10.1007/s001260050119>

Garba, I. (2000). Origin of Pan-African mesothermal gold mineralisation at Bin Yauri, Nigeria. *Journal of African Earth Sciences*, 31(2), 433-449. [https://doi.org/10.1016/S0899-5362\(00\)00098-1](https://doi.org/10.1016/S0899-5362(00)00098-1)

Garba, I. (2003). Geochemical characteristics of mesothermal gold mineralisation in the Pan-African (600±150 Ma) basement of Nigeria. *Applied Earth Science (Transaction of the Institution of Mining and Metallurgy, Section B)*, 112, 319-325

Holden, E. J., Dentith, M., & Kavesi, P. (2008). Towards the automatic analysis of regional aeromagnetic data to identify regions prospective for gold deposits. *Computer Geoscience*, 34, 1505-1513, <https://doi.org/10.1016/j.cageo.2007.08.007>

Hoover, D. B. & Pierce, H. A. (1990). *Annotated bibliography of gamma-ray methods applied to gold exploration*. U.S. Geological Survey Open-file Report, 23, 90-203.

Lawal, M. M., Salako, K. A., Abbas, M., Adewumi, T., Augie, A. I. & Khita, M. (2021). Geophysical investigation of possible gold mineralization potential zones using a combined airborne magnetic data of lower Sokoto basin and its environs Northwestern Nigeria. *International Journal of Progressive Sciences and Technologies (IJPSAT)*, 30(1), 01-16.

Lawali, S., Salako, K. A., & Bonde, D. S. (2020). Delineation of mineral potential zones over lower part of Sokoto Basin, northwestern Nigeria using aeromagnetic data. *Academic Research International*, 11(2), 19-29.

- Loke, H. M. (1999). Electrical imaging surveys for environment and engineering studies (practical guide to 2D and 3D survey). *Earth Science*, 44(1), 131–152.
- Loke, M. (2000). Rapid least-square inversion of apparent resistivity pseudosections. *Earth Science*, 64(3), 31–52.
- Lundien, J. R. (1967). *Terrain analysis by electromagnetic means: Laboratory investigations in the 0- to 2.82 – MeV gamma-ray spectral region*. U.S. Army Engineers Waterways Experiment Station, Vicksburg, Mississippi. Technical report, 41.
- Milligan, P. R. & Gunn, P. J. (1997). Enhancement and presentation of airborne geophysical data. *AGSO Journal of Australian Geology and Geophysics*, 17(2), 64–774.
- NGSA (2006). Nigerian Geological Survey Agency, Nigeria.
- Ohioma, J. O., Ezomo, F. O., & Akinsunmade, A. (2017). Delineation of Hydrothermally Altered Zones that Favour Gold Mineralization in Isanlu Area, Nigeria Using Aeroradiometric Data. *International Annals of Science*, 2(1), 20-27.
- Osazuwa, I. B., & Chii, E. C. (2010). Two-dimensional electrical resistivity survey around the periphery of an artificial lake in the precambrian basement complex of northern Nigeria. *International Journal of Physical Science*, 5(3), 238–245.
- Ramadan, T. M., & AbdelFattah, M. F. (2010). Characterization of gold mineralization in Garin Hawal area, Kebbi State, NW Nigeria, using remote sensing. *Egyptian Journal of Remote Sensing and Space Science*, 13(2), 153–163. <https://doi.org/10.1016/j.ejrs.2009.08.001>
- Sani, A. A., Augie, A. I. & Aku, M. O. (2019). Analysis of gold mineral potentials in Anka schist belt north western Nigeria using aeromagnetic data interpretation. *Journal of African Earth Sciences*, 52, 291-298.
- SARDA (1988). *Sokoto agricultural and rural development authority*. Sokoto Fadama.
- Tawey, M. D., Adetona, A. A., Alhassan, U. D., Rafiu, A. A., Salako, K. A., & Udensi, E. E. (2021). Aeroradiometric data assessment of hydrothermal alteration zones in parts of north central Nigeria. *Asian Journal of Geological Research*, 4(2), 1-16.
- Wahyu, S., Trimadona, P., & Pratomo, M. (2016). 2D Resistivity and induced polarisation measurement for manganese ore exploration. *Journal of Physics: Conference Series*, 739, <https://doi.org/10.1088/1742-6596/739/1/012138>